Chlorophyll a in Antarctic sea ice from historical ice core data

Klaus M. Meiners, Martin Vancoppenolle, S. Thanassekos, Gerhard S. Dieckmann, David N. Thomas, Jean-Louis Tison, Kevin R. Arrigo, D. L. Garrison, A. Mcminn, Delphine Lannuzel, et al.

Chlorophyll *a* in Antarctic sea ice from historical ice core data

K. M. Meiners,[1,2] M. Vancoppenolle,[3] S. Thanassekos,[4] G. S. Dieckmann,[5] D. N. Thomas,[6,7,14] J.-L. Tison,[8] K. R. Arrigo,[9] D. L. Garrison,[10] A. McMinn,[11] D. Lannuzel,[2,11] P. van der Merwe,[2,11] K. M. Swadling,[11] W. O. Smith Jr.,[12] I. Melnikov,[13] and B. Raymond[1,2]

Received 5 August 2012; revised 20 September 2012; accepted 20 September 2012; published 10 November 2012.

[1] Sea ice core chlorophyll *a* data are used to describe the seasonal, regional and vertical distribution of algal biomass in Southern Ocean pack ice. The Antarctic Sea Ice Processes and Climate – Biology (ASPeCt – Bio) circumpolar dataset consists of 1300 ice cores collected during 32 cruises over a period of 25 years. The analyses show that integrated sea ice chlorophyll *a* peaks in early spring and late austral summer, which is consistent with theories on light and nutrient limitation. The results indicate that on a circum-Antarctic scale, surface, internal and bottom sea ice layers contribute equally to integrated biomass, but vertical distribution shows distinct differences among six regions around the continent. The vertical distribution of sea ice algal biomass depends on sea ice thickness, with surface communities most commonly associated with thin ice (<0.4 m), and ice of moderate thickness (0.4–1.0 m) having the highest probability of forming bottom communities. **Citation:** Meiners, K. M., et al. (2012), Chlorophyll *a* in Antarctic sea ice from historical ice core data, *Geophys. Res. Lett.*, *39*, L21602, doi:10.1029/2012GL053478.

1. Introduction

[2] Sea ice is a major driver of Southern Ocean physics and biogeochemical cycles, and a structuring component of Antarctic marine ecosystems. Ranging in extent from 4 million km^2 in February to 19 million km^2 in September/October [*Comiso*, 2010], sea ice affects ocean-atmosphere exchange, is a reservoir of nutrients, and serves as a primer for phytoplankton blooms during ice retreat in spring [e.g., *Lannuzel et al.*, 2010; *Thomas and Dieckmann*, 2010]. Importantly, sea ice provides a habitat for ice-associated algae, which form distinct surface, interior and bottom communities [*Arrigo et al.*, 2010]. Ice algal growth is strongly controlled by physical processes. Surface communities are promoted by snow loading, surface flooding by seawater and brine, and subsequent snow-ice formation [*Fritsen et al.*, 1994, *Ackley et al.*, 2008]. In thicker sea ice, interior communities are likely to emerge following the rafting and ridging of ice floes; which are two processes that significantly contribute to the dynamical thickening of Antarctic sea ice [*Worby et al.*, 2008]. Scavenging of phytoplankton during ice formation and subsequent algal growth of incorporated algae may explain the occurrence of interior communities in frazil ice layers of un-deformed sea ice [*Arrigo et al.*, 2010]. Once established, interior communities are strongly affected by the thermodynamic sea ice regime and its phase-equilibrium which regulates percolation and convection of sea ice brines, hence controlling vertical material transport within the sea ice and across the ice-water interface [*Vancoppenolle et al.* 2010; *Saenz and Arrigo*, 2012]. Bottom communities thrive in the lowermost porous parts of sea ice floes characterized by favorable brine salinities and high nutrient availability [e.g., *Vancoppenolle et al.*, 2010].

[3] Ice algae contribute substantially to the total annual primary production of Southern Ocean ice-covered areas [*Legendre et al.*, 1992; *Lizotte*, 2001; *Arrigo et al.*, 2010]. However, these estimates, based on a limited suite of ice core data and relatively basic models, are highly uncertain, since the methods used cannot resolve the large temporal and spatial variability in ice algal distribution. In contrast to phytoplankton, sea ice algae cannot be observed from space, and the standard method to quantify ice algal biomass is to measure ice algal chlorophyll *a* (chl-a) concentrations from melted ice core sections. *Dieckmann et al.* [1998] published the first compilation of chl-a data from Antarctic ice cores collected from the Bellingshausen, Amundsen and Weddell Seas, providing vertically integrated chl-a values on ship-survey scales for the period 1983–1994. Under the auspices of the Scientific Committee on Antarctic Research (SCAR) Antarctic Sea Ice Processes and Climate (ASPeCt) program, we have significantly extended this effort to compile the first circum-Antarctic ice algal chl-a database, referred to as ASPeCt – Bio. In this study, these data are presented and used to i) identify large-scale spatial and temporal characteristics in Antarctic ice algal distribution, ii) explore

[1]Australian Antarctic Division, Department of Sustainability, Environment, Water, Population and Communities, Kingston, Tasmania, Australia.
[2]Antarctic Climate and Ecosystems Cooperative Research Centre, University of Tasmania, Hobart, Tasmania, Australia.
[3]Laboratoire d'Océanographie et du Climat (CNRS/UPMC/IRD/MNHN), IPSL, Paris, France.
[4]Commission for the Conservation of Antarctic Marine Living Resources, Hobart, Tasmania, Australia.
[5]Alfred Wegener Institute for Polar and Marine Science, Bremerhaven, Germany.
[6]School of Ocean Sciences, Bangor University, Anglesey, UK.
[7]Finnish Environment Institute, Helsinki, Finland.
[8]Laboratoire de Glaciologie, Université Libre de Bruxelles, Brussels, Belgium.
[9]Department of Environmental Earth System Science, Stanford University, Stanford, California, USA.
[10]Biological Oceanography Program, Division of Ocean Sciences, National Science Foundation, Arlington, Virginia, USA.
[11]Institute for Marine and Antarctic Studies, University of Tasmania, Hobart, Tasmania, Australia.
[12]Virginia Institute of Marine Science, College of William and Mary, Gloucester Point, Virginia, USA.
[13]P.P. Shirshov Institute of Oceanology, Russian Academy of Sciences, Moscow, Russia.
[14]Arctic Centre, Aarhus University, Aarhus, Denmark.

Corresponding author: K. M. Meiners, Australian Antarctic Division, Department of Sustainability, Environment, Water, Population and Communities, Channel Highway, Kingston, TAS 7050, Australia. (klaus.meiners@aad.gov.au)

0094-8276/12/2012GL053478

Table 1. Main Features of the ASPeCt – Bio Database

	All	DJF	MAM	JJA	SON
Number of integrated chl-a ($I_{chl\text{-}a}$) measurements	1300	134	67	425	674
$I_{chl\text{-}a}$, mean [mg m^{-2}]	6.4	12.9	8.9	3.2	6.9
$I_{chl\text{-}a}$, median [mg m^{-2}]	3.0	6.1	4.0	1.0	3.9
$I_{chl\text{-}a}$, std [mg m^{-2}]	9.9	16.5	14.2	5.9	8.9
Number of chl-a profiles[a]	990	129	57	212	592

[a]For some cores, only the integrated chlorophyll-*a* is available. The profiles correspond to a total of 8247 core sections, including 990 profiles with more than two sections. Std refers to Standard Deviation.

relationships between the physical forcings and chl-a, and iii) analyze the vertical distribution of chl-a.

2. Data Description and Methods

2.1. ASPeCt – Bio

[4] The ASPeCt – Bio dataset is a compilation of currently available sea ice chl-a data from pack ice (i.e., excluding fast ice) cores collected during 32 cruises to the Southern Ocean sea ice zone from 1983 to 2008 (Table S1 in Text S1 in the auxiliary material).[1] Data come from peer-reviewed publications, cruise reports, data repositories and direct contributions by field-research teams. During all cruises the chl-a concentration (in $\mu g\ l^{-1}$) was measured from melted ice core sections, using standard procedures, e.g., by melting the ice at <5°C in the dark; filtering samples onto glassfibre filters; and fluorometric analysis according to standard protocols [*Holm-Hansen et al.*, 1965; *Evans et al.*, 1987]. Ice samples were melted either directly or in filtered sea water, which does not yield significant differences in chl-a concentration [*Dieckmann et al.*, 1998]. The dataset consists of 1300 geo-referenced ice cores, consisting of 8247 individual ice core sections, and including 990 vertical profiles with a minimum of three sections (Table 1). The chl-a concentrations were converted to mg m^{-3} of sea ice ($C_{chl\text{-}a}$) by multiplying the value (in mg m^{-3}) of melt water by a standard sea ice to seawater density ratio (917 kg m^{-3}/1020 kg m^{-3} = 0.9). The chl-a content in mg m^{-2} ($I_{chl\text{-}a}$), that is the vertical integral of $C_{chl\text{-}a}$, is used as a proxy for the total integrated biomass.

2.2. Vertical Chl-a Distribution

[5] To analyze the vertical chl-a distribution, all profiles were linearly interpolated on a 99-layer vertical grid, conserving $I_{chl\text{-}a}$. This grid was used to (i) classify the community types (surface, internal, bottom) according to the position of the chl-a maximum and (ii) compute the percentage of $I_{chl\text{-}a}$ in the surface, internal and bottom third of the ice cores (for details see Figures S1 and S2).

2.3. Seasonal Cycle of Chl-a

[6] The seasonal cycle of $I_{chl\text{-}a}$ was analyzed relative to the 1983–2008 monthly mean seasonal cycle of NCEP air temperatures [*Kalnay et al.*, 1996] and photosynthetically available radiation (PAR) taken over the whole Antarctic sea ice zone, excluding points where satellite ice concentrations were below 15%. The computation of PAR is based on empirical formulas from *Vancoppenolle et al.* [2011], as detailed in the auxiliary material.

[1]Auxiliary materials are available in the HTML. doi:10.1029/2012GL053478.

2.4. Chl-a Profile Shape as Function of Ice Thickness

[7] In order to investigate how the shape of the chl-a profiles depends on ice thickness, the probability of the occurrence of a chl-a maximum was computed using 5 vertical core sections of equal thickness and 5 core length categories. The lower limits for each bin were chosen as: 0, 0.4, 0.7, 1 and 2 m.

3. Results and Discussion

3.1. Limitations of the Data

[8] Limitations in the dataset relate to unavoidable biases in fieldwork: sampling is not uniform across seasons, regions or ice types. More than 80% of cores were obtained during winter (June–August, JJA) and spring (September–November, SON) periods, while the summer (December–February, DJF) and autumn (March–May, MAM) periods include relatively low numbers of cores (Table 1). The spatial coverage across the six zonal sectors around Antarctica [*Worby et al.*, 2008] is also heterogeneous, with about 80% of the cores belonging to the Pacific, East Weddell and Amundsen/Bellingshausen sectors (Figure 1 and Table 2). Only 13 cores from a single voyage to the Indian sector were available (Table S1). Preferred sampling of un-deformed ice due to difficulties in accessing and extracting cores from deformed ice causes an additional bias. The ASPeCt – Bio mean ice core length generally agrees with the climatological mean ice thickness from the ASPeCt physical dataset [*Worby et al.*, 2008], both on circumpolar and regional scales (see Table 2), but underestimates thickness where deformed ice is prevalent (e.g., in the West Weddell and Ross sectors). The second limitation of the ASPeCt – Bio data arises because cell-specific ice algal chl-a content varies as a function of environmental and physiological conditions, with

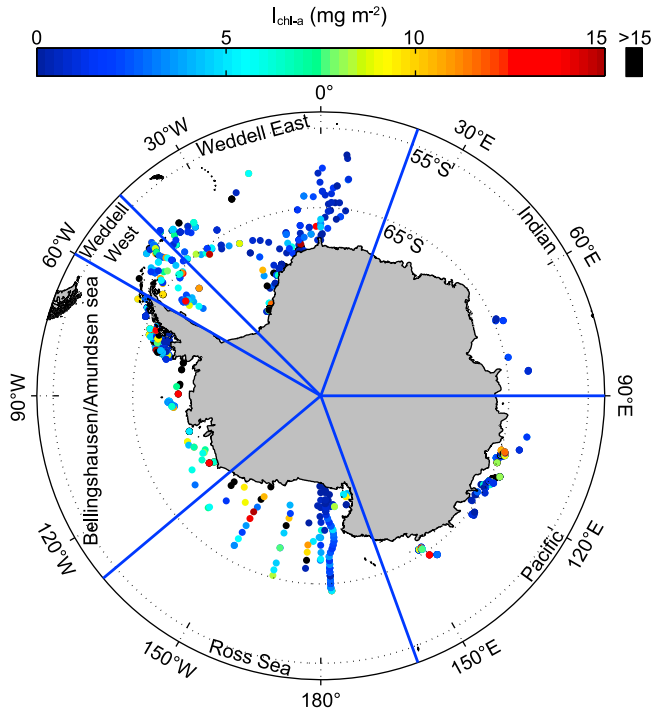

Figure 1. Map showing the location of ice cores and the associated integrated chlorophyll-*a*.

Table 2. Regional pattern of vertical distribution of assemblage type and total biomass within the sea ice cover[a]

Region	N	Surface [%]	Internal [%]	Bottom [%]	Core length [m] Mean (std)	Thickness, climatology [m][b] Mean (std)
Relative Number (%) of Profiles for Each Assemblage Type						
Circumpolar	990	27.4	16.3	56.3	0.89 (0.59)	0.87 (0.67)
Relative Contribution to Integrated Chl-a for Each Assemblage Type						
Circumpolar	990	29.2	31.4	39.4	0.89 (0.59)	0.87 (0.67)
West Weddell	124	13.9	21.1	65.0	1.22 (0.61)	1.33 (1.13)
East Weddell	242	13.3	26.0	60.7	0.90 (0.58)	0.73 (0.78)
Indian	13	13.2	25.3	61.5	0.79 (0.52)	0.68 (0.70)
Pacific	313	44.4	28.2	27.4	0.67 (0.33)	0.79 (0.87)
Ross	97	46.6	36.7	16.6	0.85 (0.36)	1.07 (1.04)
Amundsen/Bellingshausen	201	37.1	29.8	33.2	1.03 (0.84)	0.90 (0.87)

[a]The first row refers to the percentage of profiles classified as surface, internal and bottom type (for details see text). The other rows refer to the fraction of total biomass (as integrated chlorophyll-*a*) in surface, internal and bottom third of the ice cores. Profiles with less than 3 core sections are excluded.
[b]Annual mean thickness, taken from the physical ASPeCt climatology of *Worby et al.* [2008], based on 23373 observations.

diatom carbon to chl-a ratios ranging between 20 and >40 (g/g) [see *Arrigo et al.*, 2010]. Hence, chl-a is an indirect measure of ice algal biomass, and will not always accurately reflect variations across different seasons, regions and habitats, but represents the most widely available measure for ice algal distribution. Despite these limitations, the ASPeCt – Bio data represents the most comprehensive measure of Southern Ocean ice algal chl-a to date, and offers valuable insights into the seasonal development, regional characteristics and vertical structure of Antarctic ice algal distribution.

3.2. Integrated Chl-a ($I_{chl\text{-}a}$)

[9] On a circum-Antarctic scale $I_{chl\text{-}a}$ is variable, ranging from <0.1 to 89.2 mg m^{-2} with a mean of 6.4 ± 9.9 mg m^{-2} (Table 1). Low $I_{chl\text{-}a}$ values are the most common: for 49.6% of the ice cores it is below 3 mg m^{-2} and for 29.2% it is below 1 mg m^{-2}. Seasonal mean $I_{chl\text{-}a}$ is highest in summer (DJF), declines during autumn (MAM), reaches a winter minimum (JJA) and increases again in spring (SON). Median seasonal $I_{chl\text{-}a}$, less susceptible to extreme values and therefore considerably lower than the means, show a similar seasonal distribution and indicate the robustness of the observed seasonal cycle. The seasonal features in the ASPeCt – Bio dataset are consistent with regional investigations [e.g., *Fritsen et al.*, 1994; *Tison et al.*, 2008].

[10] Mean monthly $I_{chl\text{-}a}$ shows distinct increases in January, February and September (Figure 2a) and is consistent with seasonal changes in air temperature and PAR (Figures 2b and 2c). The pattern in monthly-binned data is less robust than the seasonal means because some months are poorly sampled. The increase from August to September, computed from 178 and 264 cores, respectively, is considered robust. The September increase corresponds to the onset of increase in PAR to >100 μmol quanta m^{-2} s^{-1} (Figure 2c) over the seasonally changing Antarctic sea ice zone (Figure 2d). This increase in PAR releases light limitation for ice algae, and results in a rapid biomass accumulation. The increase from December (57 cores) to January (42 cores) and February (31 cores) is based on only 130 cores and must be interpreted with caution. Decreasing temperatures in February induce vertical instability in sea ice brines, promoting nutrient re-supply due to increased exchange of brine and under-ice sea water, resulting in an ice algal autumn bloom [*Fritsen et al.*, 1994; *Vancoppenolle et al.*, 2010; *Saenz and Arrigo*, 2012]. The generally low but biologically significant $I_{chl\text{-}a}$ values in cores sampled between May and August are arguably the result of preservation of remnant ice algal chl-a and scavenged phytoplankton incorporated into the sea ice during its formation [*Garrison et al.*, 1983], in situ growth [*Melnikov*, 1998] as well as an increase in cell-specific chl-a content due to low-light adaptation of ice algae in winter.

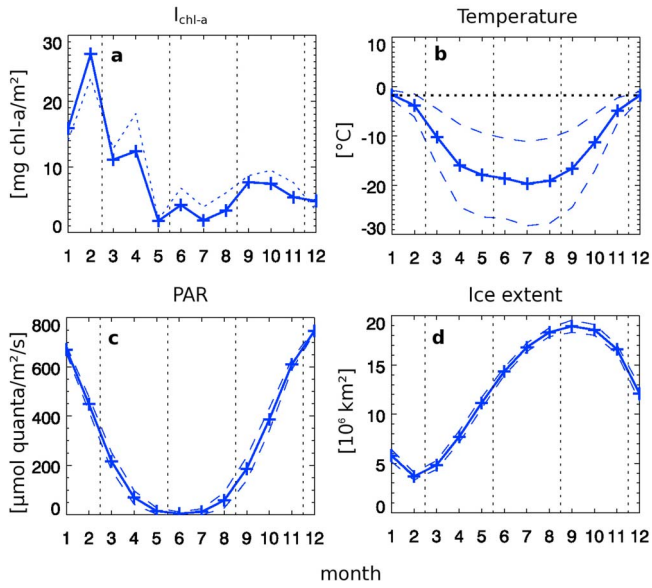

Figure 2. Seasonal cycle of (a) mean integrated chlorophyll-*a* (solid = mean, dash = standard deviation), (b) sea-ice zone average of air temperature (solid = mean, dash = mean +/− 1 standard deviation), (c) sea ice zone average of Photosynthetically Available Radiation (PAR, solid = mean, dash = mean+/− 1 standard deviation), and (d) mean seasonal ice extent (solid = mean, dash = mean+/− 1 standard deviation) from *EUMETSAT OSISAF* [2010]. Integrated chl-a is from the ASPeCt – Bio dataset. Air temperature derives from NCEP-NCAR reanalyses, PAR was computed as function of latitude, day of year, humidity and cloud fraction climatologies (see auxiliary material for details). Dotted line in Figure 2b corresponds to the seawater freezing point for a seawater salinity of 34 g kg^{-1}.

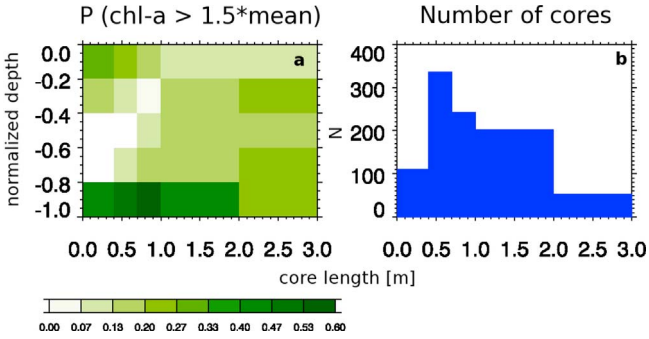

Figure 3. (a) Probability of a chlorophyll-*a* value higher than 1.5 times the vertically-integrated mean, using 5 layers and 5 core length categories. (b) Number of ice cores per core length category. See Text S1 in the auxiliary material for a description of methods.

3.3. The Vertical Distribution of Sea Ice Chl-a ($C_{chl\text{-}a}$)

[11] Mean $C_{chl\text{-}a}$ is 0.94 ± 7.29 mg m^{-3} (range 0–404.9 mg m^{-3}). More than half (56.3%) of all ice cores show biomass maxima in the bottom third, followed by 29.2% with a biomass maximum in the surface, and 16.3% in internal layers (Table 2). The bottom, internal and surface sections represent 39.4%, 31.4% and 29.3% of $I_{chl\text{-}a}$, respectively, demonstrating that on a circum-Antarctic scale, the vertical distribution of ice algal biomass is relatively even. The dataset does not show any reliable or notable seasonal evolution of the vertical distribution of ice algal biomass. Regional comparison of vertical biomass distributions shows that ice cores from the Pacific, Ross and Amundsen/Bellingshausen sectors have a relatively high contribution to $I_{chl\text{-}a}$ in the surface. In contrast, bottom communities dominate $I_{chl\text{-}a}$ in the West and East Weddell sectors, and in the poorly sampled Indian sector. Snow loading is considered to be a key driver for the development of surface and internal communities [e.g., *Ackley et al.*, 2008], but unfortunately, the ASPeCt – Bio database provides insufficient snow measurements to directly test this hypothesis. However, estimates by *Maksym and Markus* [2008] suggest that the Amundsen/Bellingshausen and Pacific sectors feature the highest relative contribution of snow-ice, which is consistent with the highest ice algal biomass in the surface (Table 2). Regional differences in atmospheric conditions may be responsible for the regional differences in ice algal vertical distribution, via their influence on snow/ice thickness ratios that determine seawater and brine flooding at the ice surface and irradiance in the ice interior and bottom layers. Atmospheric forcing may also result in differences in the relative contribution of frazil versus congelation ice types, which might affect the vertical distribution of algae, e.g. by enhanced incorporation of phytoplankton into frazil ice layers during ice formation [*Garrison et al.*, 1983; *Arrigo et al.*, 2010].

[12] The probability of the occurrence of a chl-a maximum in relation to ice thickness is shown in Figure 3a. The total number of cores in each core length bin is shown in Figure 3b. The analysis indicates that (i) thin, level ice (<0.4 m) is prone to both bottom and surface communities, (ii) thicker, level ice (0.4–1 m) is most likely to harbor bottom communities, and (iii) thick, deformed ice has more evenly distributed biomass. The probability of finding surface communities decreases monotonically with ice thickness. The high likelihood for a bottom chl-a maximum in the 0.4–1.0 m core length class is robust, as this ice core length class is the most representative, both in the ASPeCt – Bio database and in the physical ASPeCt climatology [*Worby et al.*, 2008]. This high prevalence is a result of favorable environmental conditions in the bottom horizons of this ice thickness class including high nutrient availability due to exchange with the under-ice water column, sufficient irradiance availability, and insulation against synoptic scale variations in air temperatures. The more evenly distributed maximum chl-a concentration in thicker sea ice (>1.0 m) is attributed to the fact that high thicknesses strongly imply a dynamic growth history. Rafting or ridging events randomly redistribute previously formed bottom and surface communities throughout the ice. However, it is noted that the number of ASPeCt – Bio ice cores >2 m in thickness is relatively low (Figure 3b).

[13] This analysis is the first attempt to quantify the relationship between ice thickness and the shape of Antarctic ice algal biomass profiles. Our results show that sea ice bottom biomass is not distributed evenly across ice thickness classes. In particular, 0.4–1 m thick sea ice, representing the mean Antarctic ice thickness, harbors bottom ice algal communities that provide a readily accessible food source for pelagic herbivores. Antarctic krill feed on sea ice bottom communities [e.g., *Daly*, 1990] and for some areas in the Antarctic, a positive relationship between winter sea-ice extent and krill abundance has been established [*Atkinson et al.*, 2004]. Climate models predict, on average, that Antarctic sea ice will decrease by 24% in extent and 34% in volume by the end of this century [*Arzel et al.*, 2006]. Our study suggests that the winter-spring ice thickness distribution is a key factor that will affect the vertical distribution of ice algae at the time krill need food for survival, reproduction and growth.

4. Conclusions

[14] This study provides the first observational seasonal cycle of ice algal biomass across the entire Antarctic sea ice zone. Within the limitations of the data, these provide an important baseline that is consistent with more spatially and temporally confined time-series and modeling studies. Our data suggest peaks in integrated biomass in early spring and late summer, which highlights the importance of light and nutrient availability for seasonal ice algal accumulation.

[15] Our study provides the first analysis of Antarctic sea ice chl-a profile shape and its dependence on ice thickness, and emphasizes the relatively equal contribution of surface, internal and bottom layers to biomass. The internal biomass maxima are found to be the least frequent in the ASPeCt – Bio data, but their contribution to $I_{chl\text{-}a}$ is nearly equal to those of bottom and surface communities. This suggests that these assemblages, more commonly found in under-sampled thick, deformed ice, might contribute more than previously suspected to overall chl-a biomass. Future studies need to sample complete ice core profiles in thicker ice regimes in order to improve integrated biomass estimates. In order to better understand the role that snow loading plays in ice

algal distribution, companion snow depth measurements are greatly needed. Sea ice algae models need to be multi-layered to accurately estimate ice algal primary production in Southern Ocean sea ice [e.g., *Saenz and Arrigo*, 2012]. Our study suggests that predicted changes in sea ice thickness distribution may strongly affect the vertical distribution of biomass in sea ice, with potential consequences for pelagic food webs. The sea ice scientific community is encouraged to provide further data to the ASPeCt – Bio database, which is publicly available through the Australian Antarctic Data Centre.

[16] **Acknowledgments.** We thank the ship captains, crews and our colleagues from many different countries that supported the sea ice sampling activities during the various field programs that contributed to this study. This work was carried out under the auspices of the Scientific Committee on Antarctic Research – ASPeCt program, and also contributes to the Scientific Committee on Ocean Research working group on Biogeochemical Exchange Processes at the Sea-Ice Interfaces. This work was supported by the Australian Governments Cooperative Research Centres Program through the Antarctic Climate and Ecosystems Cooperative Research Centre. Interpretations and conclusions are those of the authors and do not imply the endorsement of the National Science Foundation. We thank the reviewers for their constructive comments on an earlier draft of this paper.

[17] The Editor thanks two anonymous reviewers for their assistance in evaluating this paper.

References

Ackley, S. F., M. J. Lewis, C. H. Fritsen, and H. Xie (2008), Internal melting in Antarctic sea ice: Development of "gap layers," *Geophys. Res. Lett.*, *35*, L11503, doi:10.1029/2008GL033644.

Arrigo, K. R., T. Mock, and M. P. Lizotte (2010), Primary producers and sea ice, in *Sea Ice*, edited by D. N. Thomas and G. S. Dieckmann, pp. 283–326, Blackwell Sci., Oxford, U. K.

Arzel, O., T. Fichefet, and H. Goosse (2006), Sea ice evolution over the 20th and 21st centuries as simulated by current AOGCMs, *Ocean Modell.*, *12*, 401–415, doi:10.1016/j.ocemod.2005.08.002.

Atkinson, A., V. Siegel, E. Pakhomov, and P. Rothery (2004), Long-term decline in krill stock and increase in salps within the Southern Ocean, *Nature*, *432*, 100–103, doi:10.1038/nature02996.

Comiso, J. C. (2010), Variability and trends in global sea ice cover, in *Sea Ice*, edited by D. N. Thomas and G. S. Dieckmann, pp. 205–246, Blackwell Sci., Oxford, U. K., doi:10.1002/9781444317145.ch6.

Daly, K. L. (1990), Overwintering development, growth, and feeding of larval *Euphausia superba* in the Antarctic marginal ice zone, *Limnol. Oceanogr.*, *35*(7), 1564–1576, doi:10.4319/lo.1990.35.7.1564.

Dieckmann, G. S. et al. (1998), A compilation of data on sea ice algal standing crop from the Bellinghausen, Amundsen and Weddell Seas from 1983 to 1994, in *Antarctic Sea Ice: Biological Processes, Interactions and Variability*, *Antarct. Res. Ser.*, vol. 73, edited by M. P. Lizotte and K. R. Arrigo, pp. 85–92, AGU, Washington, D. C., doi:10.1029/AR073p0085

EUMETSAT OSISAF (2010), Global sea ice concentration reprocessing dataset 1978–2007 (v1), http://osisaf.met.no, EUMESTAT, Darmstadt, Germany.

Evans, C. A., J. E. O'Reilly, and J. P. Thomas (1987), *A Handbook for the Measurements of Chlorophyll a and Primary Production*, *BIOMASS Sci. Ser.*, vol. 8, Tex. A&M Univ., College Station.

Fritsen, C. H., V. I. Lytle, S. F. Ackley, and C. W. Sullivan (1994), Autumn bloom of Antarctic pack-ice algae, *Science*, *266*(5186), 782–784, doi:10.1126/science.266.5186.782.

Garrison, D. L., S. F. Ackley, and K. R. Buck (1983), A physical mechanism for establishing algal populations in frazil ice, *Nature*, *306*, 363–365, doi:10.1038/306363a0.

Holm-Hansen, O., C. J. Lorenzen, R. W. Holmes, and J. D. H. Strickland (1965), Fluorometric determination of chlorophyll, *ICES J. Mar. Sci.*, *30*(1), 3–15, doi:10.1093/icesjms/30.1.3.

Kalnay, E., et al. (1996), The NCEP/NCAR 40-year reanalysis project, *Bull. Am. Meteorol. Soc.*, *77*, 437–471, doi:10.1175/1520-0477(1996)077<0437:TNYRP>2.0.CO;2.

Lannuzel, D., V. Schoemann, J. de Jong, B. Pasquer, P. van der Merwe, F. Masson, J.-L. Tison, and A. Bowie (2010), Distribution of dissolved iron in Antarctic sea ice: Spatial, seasonal, and inter-annual variability, *J. Geophys. Res.*, *115*, G03022, doi:10.1029/2009JG001031.

Legendre, L., S. F. Ackley, G. S. Dieckmann, B. Gulliksen, R. Horner, T. Hoshiai, I. A. Melnikov, W. S. Reeburgh, M. Spindler, and C. W. Sullivan (1992), Ecology of sea ice biota, *Polar Biol.*, *12*(3–4), 429–444, doi:10.1007/BF00243114.

Lizotte, M. P. (2001), The contribution of sea ice algae to Antarctic marine primary production, *Am. Zool.*, *41*, 57–73, doi:10.1668/0003-1569(2001)041[0057:TCOSIA]2.0.CO;2.

Maksym, T., and T. Markus (2008), Antarctic sea ice thickness and snow-to-ice conversion from atmospheric reanalysis and passive microwave snow depth, *J. Geophys. Res.*, *113*, C02S12, doi:10.1029/2006JC004085.

Melnikov, I. A. (1998), Winter production of sea ice algae in the western Weddell Sea, *J. Mar. Syst.*, *17*, 195–205, doi:10.1016/S0924-7963(98)00038-4.

Saenz, B., and K. R. Arrigo (2012), Simulation of a sea ice ecosystem using a hybrid model for slush layer desalination, *J. Geophys. Res.*, *117*, C05007, doi:10.1029/2011JC007544.

Thomas, D. N., and G. S. Dieckmann (2010), *Sea Ice*, 2nd ed., Wiley-Blackwell, Oxford, U. K.

Tison, J. L., A. P. Worby, B. Delille, F. Brabant, S. Papadimitriou, D. N. Thomas, J. de Jong, D. Lannuzel, and C. Haas (2008), Temporal evolution of decaying summer first-year sea ice in the western Weddell Sea, Antarctica, *Deep Sea Res., Part II*, *55*(8–9), 975–987, doi:10.1016/j.dsr2.2007.12.021.

Vancoppenolle, M., H. Goosse, A. de Montety, T. Fichefet, B. Tremblay, and J.-L. Tison (2010), Modeling brine and nutrient dynamics in Antarctic sea ice: The case of dissolved silica, *J. Geophys. Res.*, *115*, C02005, doi:10.1029/2009JC005369.

Vancoppenolle, M., et al. (2011), Assessment of radiation forcing datasets for large-scale sea ice models in the Southern Ocean, *Deep Sea Res., Part II*, *58*, 1237–1249, doi:10.1016/j.dsr2.2010.10.039.

Worby, A. P., C. A. Geiger, M. J. Paget, M. L. Van Woert, S. F. Ackley, and T. L. DeLiberty (2008), Thickness distribution of Antarctic sea ice, *J. Geophys. Res.*, *113*, C05S92, doi:10.1029/2007JC004254.